

Filler Dependencies of Electrical Conductivity in Nanotube and Nanofiber Composites

Gianluca Ambrosetti,^{1,2,*} Claudio Grimaldi,^{1,†} Thomas Maeder,¹ Andrea Danani,² and Peter Ryser¹

¹*LPM, Ecole Polytechnique Fédérale de Lausanne, Station 17, CH-1015 Lausanne, Switzerland*

²*ICIMSI, University of Applied Sciences of Southern Switzerland, CH-6928 Manno, Switzerland*

We report on a model of polymer nanocomposites with fibrous fillers which explicitly considers the microscopic filler features and replicates the composites as random distributions of particles interconnected via electron tunneling. By exploiting the critical path method, we are able to obtain simple formulas, applicable to most nanotube and nanofiber composites, which allow to infer the overall composite conductivity starting from few parameters like filler volume fraction, size, and aspect-ratio. The validity of our formulation is assessed by reinterpreting existing experimental results and by extracting the characteristic tunneling length, which is mostly found within its expected value range. These results can be used practically to tailor the electrical properties of nanocomposites.

PACS numbers: 72.80.Tm, 64.60.ah, 81.05.Qk

The inclusion of nanometric conductive fillers such as carbon nanotubes [1] or nanofibers [2] into insulating polymer matrices allows to obtain electrically conductive nanocomposites with unique properties which are widely investigated and have several technological applications ranging from antistatic coatings to printable electronics [3]. A central issue in this domain is to create composites with an overall conductivity σ which can be controlled through the volume fraction ϕ , the shape of the conducting fillers, their dispersion in the polymer matrix, and the local inter-particle electrical connectedness. Understanding how these local properties affect the composite conductivity is therefore the ultimate goal of any theoretical investigation of such composites.

A common feature of most random insulator-conductor mixtures is the sharp increase of σ once a critical volume fraction ϕ_c of the conductive phase is reached. This transition is generally interpreted in the framework of percolation theory [4, 5, 6] and associated with the formation of a cluster of connected filler particles that spans the entire sample. The further increase of σ for $\phi > \phi_c$ is likewise understood as the growing of such a cluster.

In the case of composites with a polymeric matrix, the conducting particles are separated from each other by a thin polymeric layer, and the conduction between the fillers is originating from quantum mechanical tunneling processes [7, 8, 9, 10]. Tunneling has consequently been implemented in the percolation picture to explain peculiar transport properties near ϕ_c [8, 11, 12, 13]. Nevertheless, although a good understanding of the factors affecting ϕ_c exists, a formulation of $\sigma(\phi)$ for $\phi > \phi_c$ with predictive power is still missing. This especially applies to polymer composites with fillers such as nanotubes and nanofibers which have diameters which are comparable with the typical distances of tunneling. In these cases, the detailed behavior of tunneling is expected to take an explicit role in $\sigma(\phi)$ and should be taken into account.

In this Letter we address this problem by assuming that the conducting fillers form a network of globally

connected sites via tunneling processes [14]. We show that the calculated conductivity of composites with different filler aspect-ratios can be re-obtained by the critical path method, allowing for a simple analytical formula for $\sigma(\phi)$, valid for many regimes of interest, and having an explicit dependence on microscopic quantities such as the geometrical dimensions of the fillers and the tunneling length. We further show that, by reinterpreting conductivity data of real nanotubes and nanofibers composites, our formulation leads to consistent estimations of the tunneling length for these systems.

In modeling the conductor-insulator composite morphology, we treat the conducting fillers as identical impenetrable objects dispersed in a continuous insulating medium, with no interactions between the conducting and insulating phases. Furthermore, in order to describe rod-like filler particle shapes, we consider impenetrable spheroids (ellipsoids of revolution) up to the extreme prolate ($a/b \gg 1$) limit, where a and b are the spheroid polar and equatorial semi-axes respectively. Distributions of spheroids with different aspect-ratios a/b and volume fractions ϕ were generated inside a cubic cell with periodic boundary conditions via random sequential addition [15] and successively relaxed through monte-carlo (MC) sweeps [14, 16]. High density configurations were obtained by combining MC sweeps with particle inflation [14, 16]. The absence of global orientational order was verified using the nematic order parameter [17].

In considering the overall conductivity arising in such composites, we assume the spheroids of our distributions to be perfectly conductive and attribute to each spheroid pair i, j a tunneling conductance of the form [8]

$$g_{ij} = g_0 \exp\left(-\frac{2\delta_{ij}}{\xi}\right), \quad (1)$$

where ξ is the characteristic tunneling length, which measures the electron wave function decay within the polymer, and δ_{ij} is the minimal distance between the two spheroid surfaces. For spheres ($a/b = 1$), δ_{ij} is simply the

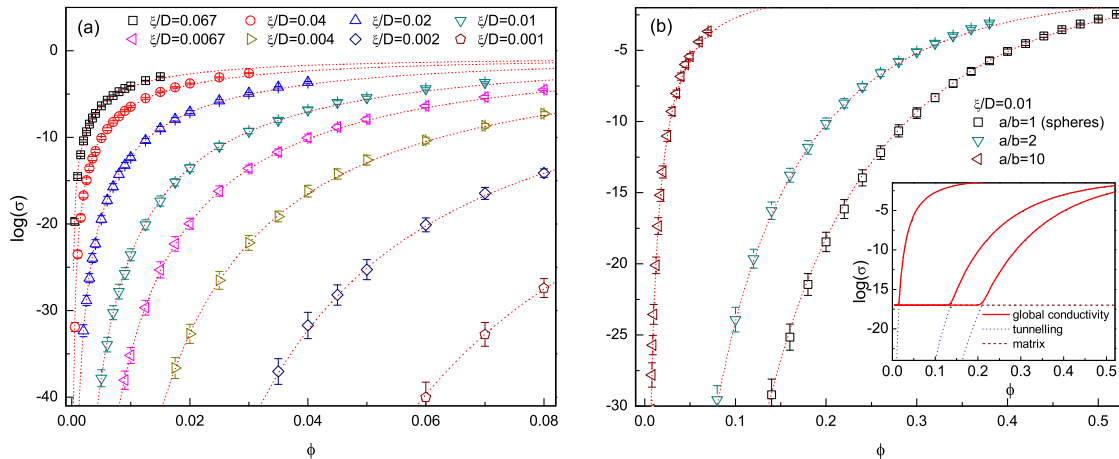


FIG. 1: (Color online) (a) Volume fraction ϕ dependence of the tunneling conductivity σ for a system of aspect-ratio $a/b = 10$ hard prolate spheroids with different characteristic tunneling distances ξ/D with $D = 2a$. Results from Eq. (2) (with $\sigma_0 = 0.179$) are displayed by dotted lines. (b) Tunneling conductivity in a system of hard prolate spheroids with different aspect-ratios a/b for the same ξ/D . Dotted lines: results from Eq. (2) with $\sigma_0 = 0.124$ for $a/b = 2$, and $\sigma_0 = 0.115$ for $a/b = 1$. Inset: schematic illustration of the tunneling conductivity crossover for the cases $a/b = 1, 2$, and 10 .

center-to-center distance minus twice the radius of the two spheres, while for the general case ($a/b \neq 1$), δ_{ij} depends also on the relative orientation of the spheroids and can be obtained from a numerical procedure described in Ref.[15]. The specific value of the pre-factor g_0 may vary for different composites and, compared to the exponential term in Eq. (1), has a weaker dependence on δ_{ij} , which we neglect by treating g_0 as a constant with unit value. We also note that in writing Eq. (1) we disregarded particle charging effects [18, 19] which, at constant room temperature, that is the case considered here, and if the particles are identical and sufficiently large, may be neglected compared to the tunneling decay.

To evaluate the global conductivity of the system, the full set of bond conductances given by equation Eq. (1) is mapped on a resistor network and the overall conductivity is calculated through numerical decimation of the resistor network [13, 20]. To reduce computational times to manageable limits, a cutoff distance δ_{co} is introduced in order to reject negligibly small bond conductances. This was typically equal to $4a$ for low density configurations, while, for spheroids at high densities, it was reduced to $\delta_{co} = 2a$ for $a/b = 1, 2$ and $\delta_{co} = a$ for $a/b = 10$.

In Fig. 1(a) we report the so-obtained conductivity σ values (symbols) as function of the volume fraction ϕ of prolate spheroids with aspect-ratio $a/b = 10$, and for different values of ξ/D , where $D = 2a$. Each symbol is the outcome of $N_R = 200$ realizations of a system of $N_P \sim 1000$ spheroids. The logarithm average of the results was considered since, due to the exponential dependence of (1), the distribution of the computed conductivities was approximately of log-normal form. The

strong reduction of σ for decreasing ϕ is a direct consequence of the fact that as ϕ is reduced, the inter-particle distances get larger, leading in turn to a reduction of the local tunneling conductances (1). Furthermore, as shown in Fig. 1(b), such reduction depends strongly on the aspect-ratio of the conducting fillers: as a/b increases, the composite conductivity drops for much lower values of ϕ for fixed ξ . However, in real composites, we have to take into account the polymer matrix whose intrinsic conductivity σ_m , which falls typically in the range $\sigma_m \simeq 10^{-13} \div 10^{-18}$ S/cm, prevents an indefinite drop of σ . This is schematically illustrated in the inset of Fig. 1(b). Now, if we identify ϕ_c with the volume fraction at which $\sigma \simeq \sigma_m$, then fillers with larger aspect-ratios entail lower values of ϕ_c , consistently with what is commonly observed. This also implies that a model of the composite conductivity based on the tunneling contribution of Eq. (1) alone will be representative only if ϕ is sufficiently larger than ϕ_c to consider the effect of σ_m negligible.

We are now going to show that the strong dependence of $\sigma(\phi)$ on a/b and ξ of Fig. 2 can be reproduced by the critical path (CP) method [21, 22] applied to our system of impenetrable spheroids. For the tunneling conductances of Eq. (1), this method amounts to keep only the subset of conductances g_{ij} having $\delta_{ij} \leq \delta_c$, where δ_c , which in turn defines the characteristic conductance $g_c = g_0 \exp(-2\delta_c/\xi)$, is the largest among the δ_{ij} distances such that the so-defined subnetwork forms a conducting cluster spanning the sample. Next, by assigning g_c to all the (larger) conductances of the subnetwork, a

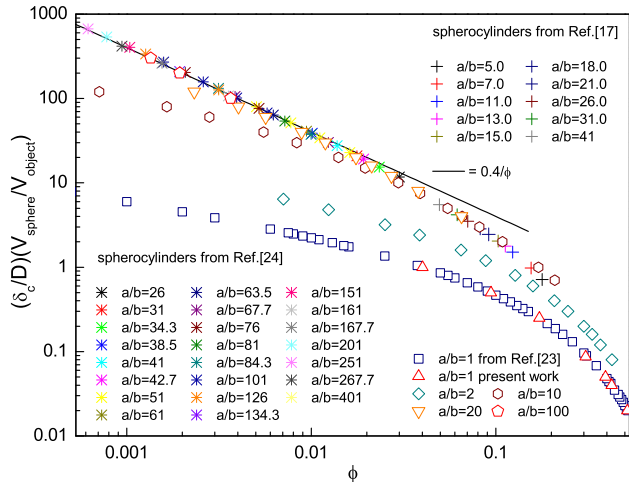


FIG. 2: (Color online) Re-scaled critical distances δ_c/D versus ϕ for the prolate spheroids with $a/b = 1, 2, 10, 20,$ and 100 , and for the impenetrable spherocylinders of Refs. [17, 24]. For $a/b = 1$ our results are plotted together with those of Ref. [23]. The solid line is the asymptotic behavior for $a/b \gg 1$.

CP approximation for σ is

$$\sigma \simeq \sigma_0 \exp \left[-\frac{2\delta_c(\phi, a, b)}{\xi} \right], \quad (2)$$

where σ_0 is a pre-factor proportional to g_0 . The significance of Eq. (2) is that it reduces the conductivity of a distribution of hard objects electrically connected by tunneling to the computation of the geometrical “critical” distance δ_c . In practice, δ_c can be obtained by coating each impenetrable spheroid of a distribution with a penetrable shell of constant thickness $\delta/2$, and by considering two spheroids as connected if their shells overlap. δ_c is then the minimum value of δ such that, for a given ϕ , a cluster of connected spheroids spans the sample. In order to illustrate the efficacy of the CP method, we have calculated δ_c for the same parameters of Fig. 1 (see below), obtaining an excellent agreement of Eq. (2) (dotted lines) with the outcomes of the full numerical decimation of the resistor network.

We shall now illustrate that for sufficiently elongated prolate spheroids, a simple relation exists that allows to estimate δ_c with good accuracy. In virtue of Eq. (2) this means that we can formulate explicit relations between σ and the shapes and concentration of the conducting fillers.

To extract δ_c we followed the route outlined in Ref. [15]. For given combinations of spheroid aspect-ratios and distance δ_c , we searched the critical (percolation) volume fraction by recording for several ϕ the probability of having a cluster spanning the opposite ends of the simulation cell, and identified it with the concentration for which this probability is equal to $1/2$. For every

configuration, we used $N_R = 40$ for the smallest values of δ_c up to $N_R = 500$ for the largest ones. The particle number varied between $N_P \sim 2000$ ($a/b = 1, 2$) and $N_P \sim 8000$ ($a/b = 100$). Relative errors on the percolation volume fraction were in the range of a few per thousand.

In Fig. 2 we report the calculated values of δ_c/D as a function of volume fraction ϕ for spheres ($a/b = 1$, together with the results of Ref. [23]), and for $a/b = 2, 10, 20,$ and 100 . In the figure, δ_c/D is multiplied by the ratio $V_{\text{sphere}}/V_{\text{object}} = (a/b)^2$, where $V_{\text{sphere}} = \pi D^3/6$ is the volume of a sphere with diameter equal to the major axis of the prolate spheroid and V_{object} is the volume of the spheroid itself. For comparison, we plot in Fig. 2 also the results for impenetrable spherocylinders of Refs. [17, 24]. These are formed by cylinders of radius R and length L , capped by hemispheres of radius R , so that $a = R + L/2$ and $b = R$, and $V_{\text{sphere}}/V_{\text{object}} = (a/b)^3/[(3/2)(a/b) - 2] \simeq (2/3)(a/b)^2$ for $a/b \gg 1$. As it is apparent, for sufficiently large values of a/b the simple re-scaling transformation collapses both spheroids and spherocylinders data into a single curve. This holds true as long as the aspect-ratio of the spheroid plus the penetrable shell $(a + \delta_c/2)/(b + \delta_c/2)$ is larger than about 5. In addition, for $\phi \lesssim 0.03$ the collapsed data are well approximated by $\delta_c(V_{\text{sphere}}/V_{\text{object}})/D = 0.4/\phi$ (solid line in Fig. 2), leading to the following asymptotic formula:

$$\delta_c/D \simeq \frac{\gamma(b/a)^2}{\phi}, \quad (3)$$

where $\gamma = 0.4$ for spheroids and $\gamma = 0.6$ for spherocylinders. Equation (3) is fully consistent with the scaling law of Ref. [25] based on the second-virial approximation for semi-penetrable spherocylinders.

We are now in the position to evaluate the tunneling driven conductivity of random distributions of prolate objects for $\sigma > \sigma_m$. By substituting Eq. (3) into Eq. (2) we obtain

$$\sigma \simeq \sigma_0 \exp \left[-\frac{2D}{\xi} \frac{\gamma(b/a)^2}{\phi} \right]. \quad (4)$$

From the previously discussed conditions on the validity of the asymptotic formulas for δ_c/D it follows that the above equation will hold when $(b/a)^2 \lesssim \phi \lesssim 0.03$. If these conditions are not met, values of δ_c can be anyway extrapolated from the data of Figs. 2.

Let us now show how the above outlined formalism may be used to re-interpret the experimental data on the conductivity of different nanocomposites with fibrous fillers that can be found in the literature. In Fig. 3(a) we report measured data of $\ln(\sigma)$ versus ϕ for polymer composites filled with Cu nanofibers [26], and carbon nanotubes [27]. Equation (2) implies that the same data can be more profitably re-plotted as a function of δ_c , instead

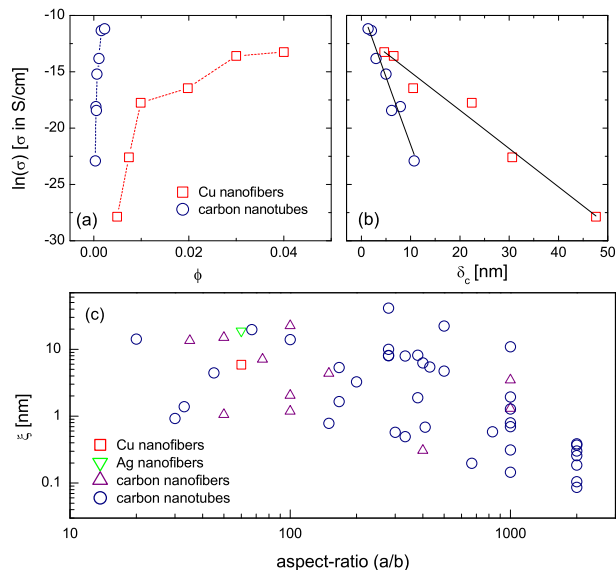


FIG. 3: (Color online) (a) Natural logarithm of the conductivity σ as a function of the volume fraction ϕ for Cu nanofibers-polystyrene[26], and single-wall carbon nanotubes-epoxy[27] composites. When, for a given concentration, more than one value of σ was given, the average of $\ln \sigma$ was considered. (b) The same data of (a) re-plotted as function of the corresponding critical distance δ_c . Solid lines are fits to Eq. (5). (c) Characteristic tunneling distance ξ values for different polymer nanocomposites as extracted by means of Eq. (5)

of ϕ . Indeed, from

$$\ln(\sigma) = -\frac{2}{\xi}\delta_c + \ln(\sigma_0), \quad (5)$$

a linear behavior with slope $-2/\xi$ is expected, independently of the specific value of σ_0 , which allows for a direct evaluation of the characteristic tunneling distance ξ . The exact value of ξ is a much investigated topic [28], and is expected to be between a fraction of nm and a few nm [8, 22, 28, 29, 30]. By using the values of D and a/b provided in Refs. [26, 27] and our formula (3) for δ_c , we find indeed an approximately linear dependence on δ_c [Fig. 3(b)], from which we extract 1.65 nm for the nanotubes, and 5.9 nm for the nanofibers.

We further applied this procedure to several published data on polymer-based nanotube [1] and nanofiber [2] composites with fillers having a/b ranging from ~ 20 up to $\sim 2 \cdot 10^3$. The results are collected in Fig. 3(c), showing that most of the so-obtained values of the tunneling length ξ are comprised between ~ 0.1 nm and ~ 10 nm. This is a striking result considering the number of factors that make a real composite deviate from an idealized model. Most notably, fillers may have non-uniform size, aspect-ratio, and geometry, they may be oriented, bent and/or coiled, and interactions with the polymer may lead to agglomeration, segregation, and sedimentation.

Furthermore, composite processing can alter the properties of the pristine fillers, e.g. nanotube or nanofiber breaking [which may explain the downward drift of ξ for high aspect-ratios in Fig. 3(c)]. In principle, deviations from ideality can be included in the present formalism by evaluating their effect on δ_c [25]. It is however interesting to notice that all these factors have often competing effects in raising or lowering the composite conductivity, and Fig. 3(c) suggests that in average they compensate each other to some extent, allowing tunneling conduction to emerge strongly from $\sigma(\phi)$ as a visible characteristic of nanocomposites.

In summary, by extending the critical path method, we have mapped the tunneling driven conductivity σ of dispersions of fibrous conducting fillers into a geometrical percolation problem, which has permitted us to formulate the filler dependencies of σ in terms of a single parameter: the critical distance δ_c . We have shown that for sufficiently large aspect-ratios of the fillers, δ_c , and so σ , can be expressed by a simple formula applicable to real dispersions of nanotubes and nanofibers. To validate our formulation, we have analyzed published conductivity data for several nanofibers and nanotube composites and extracted the corresponding values of the tunneling length ξ , which is mostly found within its expected range. The above outlined procedures can be likewise used as guidelines to tailor the electrical properties of real composites, and can be generalized to include different filler shapes, filler size and/or aspect-ratio polydispersity, and interactions with the polymer.

This study was supported by the Swiss Commission for Technological Innovation (CTI) through project GraPoly, (CTI Grant No. 8597.2), a joint collaboration led by TIMCAL Graphite & Carbon SA, and partly by the Swiss National Science Foundation (Grant No. 200021-121740). Discussions with E. Grivei and N. Johnner were greatly appreciated.

* Electronic address: gianluca.ambrosetti@epfl.ch

† Electronic address: claudio.grimaldi@epfl.ch

- [1] W. Bauhofer and J. Z. Kovacs, *Compos. Sci. Technol.* **69**, 1486 (2009).
- [2] M. H. Al-Saleh and U. Sundararaj, *Carbon* **47**, 2 (2009).
- [3] T. Sekitani, H. Nakajima, H. Maeda, T. Fukushima, T. Aida, K. Hata, and T. Someya, *Nature Mater.* **8**, 494 (2009).
- [4] M. Sahimi, *Heterogeneous Materials I. Linear Transport and Optical Properties* (Springer, New York, 2003).
- [5] D. Stauffer and A. Aharony, *Introduction to Percolation Theory* (Taylor & Francis, London 1994).
- [6] S. Kirkpatrik, *Rev. Mod. Phys.* **45**, 574 (1973).
- [7] P. Sheng, E. K. Sichel, and J. I. Gittleman, *Phys. Rev. Lett.* **40**, 1197 (1978).
- [8] I. Balberg, *Phys. Rev. Lett.* **59**, 1305 (1987).
- [9] S. Paschen, M. N. Bussac, L. Zuppiroli, E. Minder, and

- B. Hilti, *J. Appl. Phys.* **78**, 3230 (1995).
- [10] C. Li, E. T. Thorstenson, T.-W. Chou, *Appl. Phys. Lett.* **91**, 223114 (2007).
- [11] S. Vionnet-Menot, C. Grimaldi, T. Maeder, S. Strässler, and Peter Ryser, *Phys. Rev. B* **71**, 064201 (2005).
- [12] C. Grimaldi and I. Balberg, *Phys. Rev. Lett.* **96**, 066602 (2006).
- [13] N. Johner, C. Grimaldi, I. Balberg and P. Ryser, *Phys. Rev. B* **77**, 174204 (2008).
- [14] G. Ambrosetti, N. Johner, C. Grimaldi, T. Maeder, P. Ryser, and A. Danani, *J. Appl. Phys.* **106**, 016103 (2009).
- [15] G. Ambrosetti, N. Johner, C. Grimaldi, A. Danani, and P. Ryser, *Phys. Rev. E* **78**, 061126 (2008).
- [16] S. Torquato, *Random Heterogeneous Materials: Microstructure and Macroscopic Properties* (Springer, New York, 2002).
- [17] T. Schilling, S. Jungblut, and M. A. Miller, *Phys. Rev. Lett.* **98**, 108303 (2007).
- [18] P. Sheng and J. Klafter, *Phys. Rev. B* **27**, 2583 (1983).
- [19] T. Hu and B. I. Shklovskii, *Phys. Rev. B* **74**, 054205 (2006); *Phys. Rev. B* **74**, 174201 (2006).
- [20] R. Fogelholm, *J. Phys. C* **13**, L571 (1980).
- [21] V. Ambegaokar, B. I. Halperin, and J. S. Langer, *Phys. Rev. B* **4**, 2612 (1971).
- [22] B. I. Shklovskii and A. L. Efros, *Electronic Properties of Doped Semiconductors* (Springer, Berlin, 1984).
- [23] D. M. Heyes, M. Cass and A. C. Braúca, *Molec. Phys.* **104**, 3137 (2006).
- [24] L. Berhan and A. M. Sastry, *Phys. Rev. E* **75**, 041120 (2007).
- [25] A. V. Kyrilyuk, P. van der Schoot, *Proc. Natl. Acad. Sci. USA* **105**, 8223 (2008).
- [26] G. A. Gelves, B. Lin, U. Sundararaj, and J. A. Haber, *Adv. Funct. Mater.* **16**, 2423 (2006).
- [27] M. B. Bryning, M. F. Islam, J. M. Kikkawa, and A. G. Yodh, *Adv. Mater.* **17**, 1186 (2005).
- [28] R. E. Holmlin, R. Haag, M. L. Chabinyk, R. F. Ismagilov, A. E. Cohen, A. Terfort, M. A. Rampi, and G. M. Whitesides, *J. Am. Chem. Soc.* **123**, 5075 (2001).
- [29] C. H. Seager and G. E. Pike, *Phys. Rev. B* **10**, 1435 (1974).
- [30] J. M. Benoit, B. Corraze, and O. Chaurez, *Phys. Rev. B* **65**, 241405(R) (2002).